2010 3rd International Conference on Computer and Electrical Engineering (ICCEE 2010)
IPCSIT vol. 53 (2012) © (2012) IACSIT Press, Singapore
DOI: 10.7763/IPCSIT.2012.V53.No.2.36

Numerical Simulation of Production Performance of Fractured Horizontal Wells Considered Conductivity Variation

Shen Rui[+] and Gao Shusheng

Institute of Porous Flow and Fluid Mechanics, Chinese Academy of Science

Langfang, Hebei, China

Abstract—Fractured horizontal wells are widely used in the development of low permeability reservoirs at present. As well known, the conductivity of the hydraulic fracture varies with time. Therefore, this effect should be considered in the numerical simulation of low permeability reservoirs developed by fractured horizontal wells. The black oil model was improved in the paper, and the relation of the hydraulic fracture conductivity changing with time was considered in the model. The mathematical model was discretized by the finite-difference approximation, and the control equations of percolation were solved by the implicit pressure explicit saturation method. Results show the fracture conductivity has great influences on pressure distributions. In the initial stage of simulation, pressure contours near fractured wells is oval. When the fracture conductivity disappears, pressure contours near wells is circular shape.

Keywords- fractured wells;numerical simulation; fluid-solid coupling; stress sensitivity; fracture conductivity

1. Introduction

As the development of horizontal well drilling skill and fracturing technology, the application of fracturing to horizontal well became the new direction of reservoir development. The applied effect in Daqing and Changqing oil-field shows the oil production of fracturing horizontal wells is about 3~6 times to the one of near vertical wells. So the effect of the increase production is very obvious.

Currently, the conventional method of productivity prediction of fractured horizontal wells is analytical or numerical. On the one hand, the analytical method is for steady flow of single phase fluid, and it can't predict the productivity of tow-phase fluid. Therefore, it can't replace the numerical method in productivity prediction. On the other hand, the production obtained by the analytical method is under the steady state, while the flow in low permeability reservoirs is difficulty to forming the steady state in fact. So the numerical method is more accurately reflect the production performance of fractured horizontal wells. [1~4]

M.E. Villegas researched the numerical simulation method that the production performance of Longitudinal fractured wells in high permeability reservoirs [5, 6].

Karche discussed the production analysis method of fractured horizontal wells in quasi-steady flow state. He developed a numerical simulator and discussed the effect of the number of infinite-conductivity fractures on production capacity [7].

Y.Q. He built a 2-D model of reservoir and fracture. The productivity prediction method of fractured vertical wells which considered the conductivity changing with time was studied [8].

[+] Corresponding author.
E-mail address: shenrui523@126.com

H.P. Miao divided the forecast period into three stages in predicting the production of multiple fractures. It made the computational complexity decreasing significantly. The essence is that calculating production of multiple fractures by numerical method in early stage and by analytical method in middle and late stage [9].

Y. Zhang treated the reservoir and the fracture as a whole system, and simulated by the black oil simulator. But the method could not do the scheme optimization of the fracturing treatment [10].

On the basis of the previous research, reservoirs and fractures were treated as a whole flow system, and the factor of the conductivity of fractures changing with time was considered. It improved the production performance simulating precision of fractured horizontal wells.

2. Mathematical model

2.1. The 3-D Control Equation of Oil-water Two Phases

The control equation of oil phase:

$$\frac{\partial}{\partial x}\left(\frac{KK_{ro}\rho_o}{\mu_o}\frac{\partial p_o}{\partial x}\right)+\frac{\partial}{\partial y}\left(\frac{KK_{ro}\rho_o}{\mu_o}\frac{\partial p_o}{\partial y}\right)+\frac{\partial}{\partial z}\left(\frac{KK_{ro}\rho_o}{\mu_o}\frac{\partial p_o}{\partial z}\right)=\frac{\partial}{\partial t}(\rho_o\phi S_o) \tag{1}$$

The control equation of water phase:

$$\frac{\partial}{\partial x}\left(\frac{KK_{rw}\rho_w}{\mu_w}\frac{\partial p_w}{\partial x}\right)+\frac{\partial}{\partial y}\left(\frac{KK_{rw}\rho_w}{\mu_w}\frac{\partial p_w}{\partial y}\right)+\frac{\partial}{\partial z}\left(\frac{KK_{rw}\rho_w}{\mu_w}\frac{\partial p_w}{\partial z}\right)=\frac{\partial}{\partial t}(\rho_w\phi S_w) \tag{2}$$

The auxiliary equations are:

$$S_o+S_w=1 \tag{3}$$

$$p_o=p_w+p_c \tag{4}$$

$$K_{ro}=K_{ro}(S_o) \tag{5}$$

$$K_{rw}=K_{rw}(S_w) \tag{6}$$

$$\phi=\phi_0\left(1+C_f\left(p-p_0\right)\right) \tag{7}$$

$$\rho_l=\rho_l^0\left(1+C_l\left(p-p_0\right)\right) \tag{8}$$

Outer boundary conditions are：

$$\left.\frac{\partial p}{\partial x}\right|_{x=0}=\left.\frac{\partial p}{\partial x}\right|_{x=L_x}=0 \tag{9}$$

$$\left.\frac{\partial p}{\partial y}\right|_{y=0}=\left.\frac{\partial p}{\partial y}\right|_{y=L_y}=0 \tag{10}$$

$$\left.\frac{\partial p}{\partial z}\right|_{z=0}=\left.\frac{\partial p}{\partial z}\right|_{z=L_z}=0 \tag{11}$$

When the production well produced with the constant pressure, the inner boundary conditions are P_{wf}=C.

The model of horizontal wells is treated by the Peaceman method:

$$q_{sc}=\frac{-2\pi K\Delta\left(p_{i,j,k}-p_{wf}\right)}{\mu\left[\ln\left\{\frac{\left[\left(K_x/K_z\right)^{1/2}(\Delta z)^2+\left(K_z/K_x\right)^{1/2}(\Delta x)^2\right]^{1/2}}{\left(K_x/K_z\right)^{1/4}+\left(K_z/K_x\right)^{1/4}}\right\}-\ln(r_w)\right]} \tag{12}$$

where, $K=\left(K_xK_z\right)^{1/2}$.

The initial conditions are:

$$p\left(x,y,z,t\right)\big|_{t=0}=p_i \tag{13}$$

$$S_w\left(x,y,z,t\right)\big|_{t=0}=S_{wi} \tag{14}$$

2.2. The Treatment of Conductivity of Fractures

The width of fracture is very small, but the permeability is very high. Fluid flowing from formation to fractures accounts a high proportion. It would cause coefficient matrix not to converge in the numerical simulation. So grids where fractures locate should be enlarged. In the principle of flow being constant, the enlargement of grids is both suited to numerical calculation and the law of flow in porous media. To keep the equivalence of the grid, the conversion should satisfy the following equation.

$$K_f = \frac{K_{fr} \times w_{fr}}{w_f} \tag{15}$$

Previous researches show the conductivity of the sand packed fracture should decrease after fracturing. Therefore, the numerical simulation of the production performance of fractured horizontal wells should be considered this phenomenon. If the relationship between conductivity and time is considered, numerical simulation could be closer to the actual situation.

According to previous studies, the relation between conductivity and time can be described by [11,12]:

$$K_f = F_{RCD}(t) / w_f = \left[F_{RCD0} - \alpha(1+\lg t) \right] \Big/ w_f \tag{16}$$

3. Calculation methods and Numerical examples

3.1. Calculation Methods

The mathematical model is discretized by the finite-difference approximation, and the control equations of percolation are solved by the IMPES (implicit pressure explicit saturation) method:

$$\begin{aligned}
&\frac{\partial}{\partial x}\left(\lambda_{ox}\frac{\partial p_o}{\partial x}\right)+\frac{\partial}{\partial y}\left(\lambda_{oy}\frac{\partial p_o}{\partial y}\right)+\frac{\partial}{\partial z}\left(\lambda_{oz}\frac{\partial p_o}{\partial z}\right)=\frac{1}{\Delta x_i}\left[\left(\lambda_{ox}\frac{\partial p_o}{\partial x}\right)_{i+\frac{1}{2},j,k}-\left(\lambda_{ox}\frac{\partial p_o}{\partial x}\right)_{i-\frac{1}{2},j,k}\right]\\
&+\frac{1}{\Delta y_i}\left[\left(\lambda_{oy}\frac{\partial p_o}{\partial y}\right)_{i,j+\frac{1}{2},k}-\left(\lambda_{oy}\frac{\partial p_o}{\partial y}\right)_{i,j-\frac{1}{2},k}\right]+\frac{1}{\Delta z_i}\left[\left(\lambda_{oz}\frac{\partial p_o}{\partial z}\right)_{i,j,k+\frac{1}{2}}-\left(\lambda_{oz}\frac{\partial p_o}{\partial z}\right)_{i,j,k-\frac{1}{2}}\right]\\
&=\frac{2\lambda_{ox(i+\frac{1}{2})}}{\Delta x_i(\Delta x_i+\Delta x_{i+1})}\left(p_{o(i+1,j,k)}-p_{o(i,j,k)}\right)+\frac{2\lambda_{ox(i-\frac{1}{2})}}{\Delta x_i(\Delta x_i+\Delta x_{i-1})}\left(p_{o(i-1,j,k)}-p_{o(i,j,k)}\right)\\
&+\frac{2\lambda_{oy(j+\frac{1}{2})}}{\Delta y_j(\Delta y_j+\Delta y_{j+1})}\left(p_{o(i,j+1,k)}-p_{o(i,j,k)}\right)+\frac{2\lambda_{oy(j-\frac{1}{2})}}{\Delta y_j(\Delta y_j+\Delta y_{j-1})}\left(p_{o(i,j-1,k)}-p_{o(i,j,k)}\right)\\
&+\frac{2\lambda_{oz(k+\frac{1}{2})}}{\Delta z_k(\Delta z_k+\Delta z_{k+1})}\left(p_{o(i,j,k+1)}-p_{o(i,j,k)}\right)+\frac{2\lambda_{oz(k-\frac{1}{2})}}{\Delta z_k(\Delta z_k+\Delta z_{k-1})}\left(p_{o(i,j,k-1)}-p_{o(i,j,k)}\right)
\end{aligned} \tag{17}$$

$$\begin{aligned}
&\frac{\partial}{\partial x}\left(\lambda_{wx}\frac{\partial p_w}{\partial x}\right)+\frac{\partial}{\partial y}\left(\lambda_{wy}\frac{\partial p_w}{\partial y}\right)+\frac{\partial}{\partial z}\left(\lambda_{wz}\frac{\partial p_w}{\partial z}\right)=\frac{1}{\Delta x_i}\left[\left(\lambda_{wx}\frac{\partial p_w}{\partial x}\right)_{i+\frac{1}{2},j,k}-\left(\lambda_{wx}\frac{\partial p_w}{\partial x}\right)_{i-\frac{1}{2},j,k}\right]\\
&+\frac{1}{\Delta y_i}\left[\left(\lambda_{wy}\frac{\partial p_w}{\partial y}\right)_{i,j+\frac{1}{2},k}-\left(\lambda_{wy}\frac{\partial p_w}{\partial y}\right)_{i,j-\frac{1}{2},k}\right]+\frac{1}{\Delta z_i}\left[\left(\lambda_{wz}\frac{\partial p_w}{\partial z}\right)_{i,j,k+\frac{1}{2}}-\left(\lambda_{wz}\frac{\partial p_w}{\partial z}\right)_{i,j,k-\frac{1}{2}}\right]\\
&=\frac{2\lambda_{wx(i+\frac{1}{2})}}{\Delta x_i(\Delta x_i+\Delta x_{i+1})}\left(p_{w(i+1,j,k)}-p_{w(i,j,k)}\right)+\frac{2\lambda_{wx(i-\frac{1}{2})}}{\Delta x_i(\Delta x_i+\Delta x_{i-1})}\left(p_{w(i-1,j,k)}-p_{w(i,j,k)}\right)\\
&+\frac{2\lambda_{wy(j+\frac{1}{2})}}{\Delta y_j(\Delta y_j+\Delta y_{j+1})}\left(p_{w(i,j+1,k)}-p_{w(i,j,k)}\right)+\frac{2\lambda_{wy(j-\frac{1}{2})}}{\Delta y_j(\Delta y_j+\Delta y_{j-1})}\left(p_{w(i,j-1,k)}-p_{w(i,j,k)}\right)\\
&+\frac{2\lambda_{wz(k+\frac{1}{2})}}{\Delta z_k(\Delta z_k+\Delta z_{k+1})}\left(p_{w(i,j,k+1)}-p_{w(i,j,k)}\right)+\frac{2\lambda_{wz(k-\frac{1}{2})}}{\Delta z_k(\Delta z_k+\Delta z_{k-1})}\left(p_{w(i,j,k-1)}-p_{w(i,j,k)}\right)
\end{aligned} \tag{18}$$

In the Nth time step, the pressure distribution is solved by the implicit solution method. By substitution of the pressure and time data of the Nth time step into (16), the conductivity of the fracture would be calculated. Then the new distribution of permeability is used in the calculation of the (N+1)th time step.

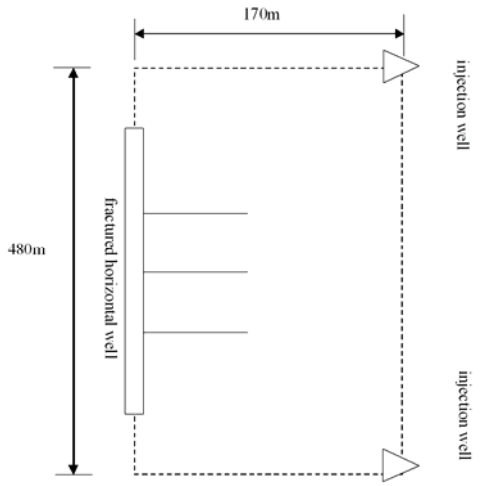

Fig.1. Schematic diagram of physical model

3.2. Calculation Methods

Fig. 1 is the schematic diagram of the reservoir developed by fractured wells. The simulated zone is the 1/2 units of the five-spot patterns, and positions of wells are shown in Fig.1. The triangle is the position of vertical injection wells. The well spacing is 480m, and the distance between two rows is 170m.

The average permeability of reservoir matrix is $1\times10^{-3}\mu m^2$, the initial formation pressure is 28 MPa, and the effective thickness is 10m. The number of grids is 33×18×1=594. The dimension of grids with fractures and wells is 10m×1m×10m. The horizontal production well is fractured, and the half-length of the fracture is 100m. The production well produces by the constant pressure and the injection well injects by the constant flow rate.

4. Results analysis

Fig.2 and Fig.3 show the pressure distribution of improved black oil simulator at t=365d and t=3650d. The pressure contours near the horizontal well was convex at t=365d. But the conductivity of fracture depleted at t=680d, so the pressure contours near the horizontal well became roughly oval at t=3650.

Therefore, the change of hydraulic fracture conductivity has great influences on the distribution of pressure.

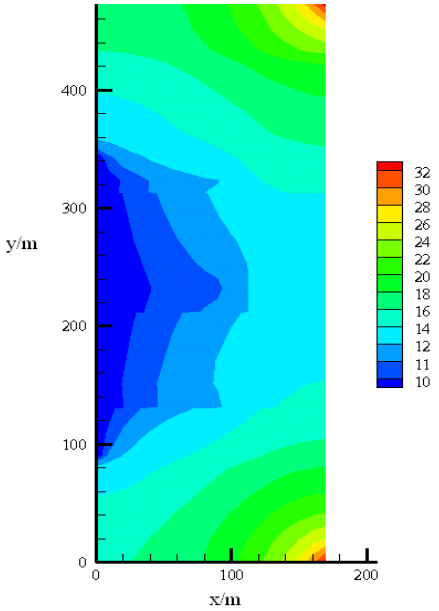

Fig.2. Pressure distribution simalated by improved black oil simulator

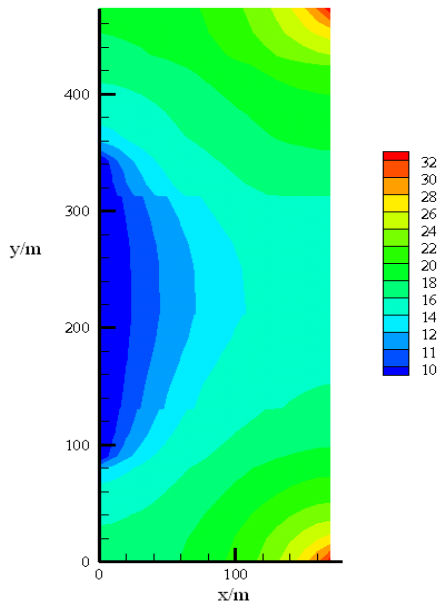

Fig.3. Pressure distribution simalated by conventional black oil simulator

5. Conclusion

According to the experiment on the conductivity of hydraulic fractures, the black oil simulator was improved by the relationship between fracture conductivity and time. The regularity of pressure distribution was studied by the improved black oil simulator.

The fracture conductivity has great influences on pressure distributions. In the initial stage of simulation, pressure contours near fractured wells is convex. When the fracture conductivity disappears, pressure contours near wells is ovality.

6. Nomenclature

P_o oil phase pressure, $ML^{-1}T^{-2}$
P_w water phase pressure, $ML^{-1}T^{-2}$
P_c capillary pressure, $ML^{-1}T^{-2}$
P_{wf} bottom hole pressure, $ML^{-1}T^{-2}$
q_{sc} production of horizontal well, L^3T^{-1}
μ_o viscosity of oil, $ML^{-1}T^{-1}$
μ_w viscosity of water, $ML^{-1}T^{-1}$
ρ_l density of fluid, ML^{-3}
S_o, oil saturation,%
S_w, water saturation,%
K absolute permeability, L^2
K_{ro}, K_{rw} relative permeability, %
K_f permeability of fracture in simulation, L^2
K_{fr} permeability of fractures, L^2
w_f width of fracture in simulation, L
w_{fr} width of fracture, L
C_l, compressibility of fluid, $M^{-1}LT^2$
C_f compressibility of rock, $M^{-1}LT^2$
L_x ,L_y length and width of reservoirs, L
h thickness of reservoirs, L
Φ porosity, dimensionless

7. References

[1] C.M. Pearson, M.D. Clonts, N.R. Vaughn, “Use of longitudinally fractured horizontal wells in a multi-zone sandstone formation”, SPE Annual Technical Conference and Exhibition, pp. 371-380, October 1996.

[2] T.M. Hegre, L. Larsen, “Productivity of multifractured horizontal wells”, European Petroleum Conference, pp. 393-404, October 1994.

[3] L. Larsen, T.M. Hegre, “Pressure transient analysis of multifractured horizontal wells”, SPE Annual Technical Conference and Exhibition, pp. 265-276, September 1994.

[4] J.E. Brown, M.J. Economides, “An analysis of hydraulically fractured horizontal wells”, SPE Rocky Mountain Regional Meeting, pp. 143-154, May 1992.

[5] M.E. Villegas, R.A. Wattenbarger, P. Valko, “Performance of longitudinally fractured horizontal wells in high-permeability anisotropic formations”, SPE Annual Technical Conference and Exhibition, pp. 371-380, October 1996.

[6] M.E. Villegas, R.A. Wattenbarger, P. Valko, M.J. Economides, “Performance of longitudinally fractured horizontal wells in high-permeability anisotropic formations”, SPE Annual Technical Conference and Exhibition, pp. 363-370, October 1996.

[7] B.J. Karcher, F.M. Giger, J. Combe, “Some practical formulas to predict horizontal well behavior”, SPE Annual Technical Conference and Exhibition, pp. 1-12 . October 1986.

[8] Y.Q. He, H.X. Wang, “Prediction of production performance in fractured wells with numerical simulation”, Journal of University of Petroleum, Vol. 14, October 1990, pp. 16-25.

[9] H.P. Miao, H.X. Wang, “Optimization of the number of fractures and production forecast of horizontal wells after fracturing”, Oil Drilling & Production Technology, Vol. 14, December 1992, pp. 51-56.

[10] Y. Zhang, “Production forecast and its application of horizontal and extended reach wells after fracturing”, Chengdu: Southwest Petroleum University, 2003, pp. 14-26.

[11] Q.Z Wen, S.C. Zhang, L. Wang, Y.S. Liu, “Influence of propping embedment on fracture long-term flow conductivity”, Nature Gas Industry, Vol. 25, August 2005, pp.65-68.

[12] Q.Z Wen, S.C. Zhang, X.Y. Wang, S.W. Zhu, “Numerical calculation of long-term conductivity of propping fractures”, Oil Drilling & Production Technology, Vol. 27, August 2005, pp. 68-71.